DYNAMIC CHARACTERISTICS OF PLATFORM WITH SMA HELICAL SPRING SUSPENSION

Chun-Ying Lee*[1], Chao-Sung Lin[2] and Huan-Chang Zhuo[1]

[1]Department of Mechanical and Automation Engineering, Da-Yeh University
Da-Tsuen, Changhua 515, Taiwan
[2]Department of Materials Science and Engineering, National Taiwan University
Taipei 106, Taiwan
leech@mail.dyu.edu.tw

Abstract

The platform with vibration isolation suspension is frequently used in the high precision machinery. When the component mounted on the platform generates periodic oscillation due to parametric excitation, e.g. rotation of an eccentric mass, the induced vibration of the platform, especially near the resonance, could undermine the functionality of the platform. The dynamic characteristics of a platform supported with four SMA suspension springs were investigated in this study. The SMA spring undergoes phase transformation reversibly from martensite to austenite as the temperature is raised. In the meanwhile, the elastic modulus of the austenite phase is different from that of martensite. Therefore, by controlling the temperature of the suspension SMA springs, the resonance frequency of the platform can be actively tuned. The spring constant of the helical spring in transverse deformation was derived by employing Castigliano's theorem. The derived spring constant was justified by the finite element analysis of ANSYS. Consequently, the spring constant measurements both from static and vibration setups were used in the theoretical equations to infer the equivalent elastic modulus of the SMA at different temperatures. Finally, the dynamic tuning capability of the platform was demonstrated experimentally. It was found that both the resonance frequency and damping for in-plane vibration mode of the platform could be tuned within 20% and 200% of variation respectively, as the temperature of the springs was changed between 25°C and 90°C.

INTRODUCTION

The increasing demand for the high precision machinery with better performance has offered the engineers with challenges in suppression of vibration. For example, the

pursuit of higher and higher read/write speed of optical disk drive has rendered the solutions of a variety of vibration suppression techniques. For an optic disk drive platform with imbalanced mass, the centrifugal force generated by the high speed rotation of the disk induces the vibration of the platform. For the common practice, the suspension springs are consisted of metallic spring washer or rubber ring. The dynamic characteristics of the washer can be optimally tuned for certain operation condition to minimize the induced vibration. However, the disk drive usually reads or writes in different speeds. Thus, the tuning of the washer becomes difficult for minimizing the vibration in all operational conditions.

Another category of vibration reduction device used in the commercial optic disk drive is the ball balancer [1-3]. Basically, the freely movable balls in the circular tracks are automatically driven to their counterbalance positions which centre of mass is in 180-degree, opposite side, to the imbalanced mass. These balls generate counterbalance force to cancel the centrifugal force due to the imbalanced mass. The induced vibration is therefore reduced. However, the ball balancer device only works for the rotation speed exceeding the critical speed of the platform. It will not help to reduce the vibration if the rotational speed is lower than the natural frequency of the platform [1, 4].

Shape memory alloy (SMA), along with other smart materials, can change its material properties under the influence of control parameter. For instance, electrorheological (ER) fluid undergoes phase transition from viscous liquid to Bingham plastic with the application of electric field. The idea of using suspension washer with embedded ER fluid for the optic disc drive platform was demonstrated to be capable of tuning the platform's natural frequency with applied electric field [5]. On the other hand, the Young's modulus of the SMA increases from martensite to austenite with the actuation of heat and/or strain. The composite beam with embedded SMA wires [6], vibration absorber in the form of cantilever SMA beam [7], and compression helical spring [8], etc. are some examples of employing the tunable property of the SMA in the literature. Although the application of SMA spring in the semi-active vibration control is not unseen, the spring washer used in the optic disk drive platform for the same purpose is new. The helical spring in this application is subjected to transverse deformation in contrast to axial or torsion deformation for usual designs. Therefore, the spring constant of a helical spring in transverse loading was formulated in this study. The variation of the spring constant with respect to the controlled temperature was also measured experimentally. Finally, the tunable resonance frequency and damping capacity of the platform with four suspension SMA springs were demonstrated.

THEORETICAL FORMULATION

Since the rotation of the suspension spring was restrained at the end of the platform, a single helical spring subjected to transverse loading with constrained end rotation was firstly considered in this study. Figure 1 illustrates the geometric configuration and associate end reactions of the helical spring. The material was

assumed to be elastic in nature. Thus, the Castiliano's Theorem can be used to derive the spring constant of the linear spring.

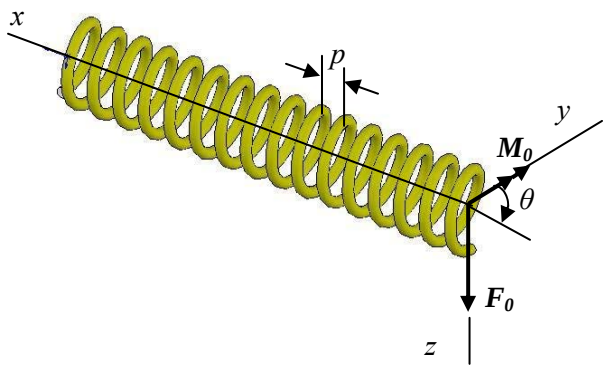

Figure 1 -- Helical spring subjected to lateral loading with its ends restrained in transverse rotation.

In Fig. 1, the $\boldsymbol{F}_0$ and $\boldsymbol{M}_0$ denote the transverse loading and the end moment reaction, respectively. The reaction moment $\boldsymbol{M}_0$ was induced to maintain the zero rotation at the end. p is the pitch, r is the mean helical radius and θ is polar coordinate of the spring. The coordinate function of the central line of the helical spring can be written as:

$$x = r\cos\theta, y = r\sin\theta, z = \frac{\theta}{2\pi}p \tag{1}$$

By taking the derivatives of the above coordinates, we can find the unit tangent vector to the helical line:

$$\vec{e}_t = \frac{1}{\sqrt{r^2 + \frac{p^2}{4\pi^2}}}\left(-r\sin\theta\vec{i} + r\cos\theta\vec{j} + \frac{p}{2\pi}\vec{k}\right) \tag{2}$$

The reactions at a cross-section θ to satisfy the equilibrium of a free body diagram can be obtained as:

$$\vec{F} = F_0\vec{j} \tag{3a}$$

$$\vec{M} = M_0\vec{i} + \vec{r}\times\vec{F}\,, \tag{3b}$$

where $\vec{r}$ is the position vector as following:

$$\vec{r} = -r\cos\theta\vec{i} + (r - r\sin\theta)\vec{j} - \frac{p}{2\pi}\theta\vec{k} \tag{4}$$

Accordingly, the reaction force in Eqn. (3a) can be resolved into axial and transverse components P and V, which are axial force and shear force, respectively. Similarly, the moment in Eqn.(3b) can be resolved into twisting torque T and bending moment M in the wire.

$$P = \vec{F}\bullet\vec{e}_t\,,\ V = \sqrt{\left|\vec{F}\right|^2 - P^2} \tag{5a}$$

$$T = \vec{M}\bullet\vec{e}_t\,,\ M = \sqrt{\left|\vec{M}\right|^2 - T^2} \tag{5b}$$

Under the assumptions of linear structure and small axial and transverse shear deformations, the total strain energy U can be obtained by integrating the strain energy density associated with twisting and bending deformations over the length of the wire:

$$U = \int_0^{2N_c\pi} \left(\frac{M^2}{2EI} + \frac{T^2}{2GJ} \right) r d\theta \tag{6}$$

Because the end of the spring is constrained in angular rotation (θ_0=0), the following equation can be written by adopting the Castigliano's Theorem:

$$\theta_0 = \frac{\partial U}{\partial M_0} = 0 \tag{7}$$

Eqn.(7) is the equation relating the reactive moment M_0 to the applied loading F_0 at the end of the spring. Substituting the resulted relationship back into Eqn.(6) and applying the Castigliano's Theorem again, we can derive the lateral deflection of the spring at the end:

$$\delta = \frac{\partial U}{\partial F_0} \tag{8}$$

With the result in Eqn.(8), the spring constant can be obtained subsequently.

$$k = \frac{F_0}{\delta} \tag{9}$$

For the case of spring with freely rotated end, the result can be applied by setting the constraint moment M_0 to zero. If a concentrated mass m is mounted at the end of a helical spring and the other end of the spring is fixed, then the natural frequency of the spring-mass system can be found by:

$$f = \frac{\omega}{2\pi} = \frac{1}{2\pi}\sqrt{\frac{k}{m}} \tag{10}$$

EXPERIMENTAL MEASUREMENTS AND DISCUSSIONS

Before we proceeded to experimental study, the formulation described in the previous section was first justified by a numerical analysis using ANSYS. The spring with r=3.5mm, d=1mm, N_c=10, E=23.8GPa, G=9.17GPa was subjected to a lateral load 3.342N. The finite element model was built employed 3D beam element. Both the results of ANSYS model and the present formulation are presented in Table 1. The less than 1% difference between these two results justifies the formulation presented herein.

The SMA spring used in this study was a commercial product distributed by Jameco Electronics. The mean diameter of the coil and the diameter of the wire are 7mm and 1mm, respectively. Due to the unavailability of the material property, an axial

Table 1-- The lateral deflection and spring constant of a helical spring subjected to transverse loading and end rotation constraint

	ANSYS model	Present formulation	Difference(%)
Lateral deflection(*mm*)	0.685	0.6838	0.175
Spring constant (*kN/mm*)	4.879	4.887	0.175

loading testing apparatus was set up to study the phase transformation characteristics of the SMA spring. The SMA spring was loaded in between two Teflon insulating spacers. The insulating spacers confined the electric current only thru the spring to raise its temperature via ohmic effect. A control module controlled the current supply and the temperature was monitored by a thermocouple. As to the measurement of mechanical loading and the associate deflection, the deflection was imposed by adjusting the clamped length of the micrometer while the serial connected load cell kept recording the corresponding compressive loading. The slope of the measured load-deflection curve gave the spring constant of the spring at various controlled temperatures.

The measured spring constant of the axially loaded SMA spring was employed to inferred the equivalent Young's modulus from the design formula of helical spring $k=Gd^4/64R^3N_c$ and $E=2(1+v)G$. The obtained Young's modulus at different temperatures in the heating and followed cooling process is shown in Fig. 2. Before any measurement started, the SMA spring was quenched in the liquid nitrogen to fully recover to martensitic phase. As the temperature was raised to 30°C, the Young's modulus increased. This could be caused by the work-hardening of the virgin martensite after the first loading test at room temperature. As the temperature was further raised, the modulus decreased to a minimum at 40°C and increased to a saturated magnitude near 90°C. The decrement and increment of the modulus during the heating process should be obliged to the yielding of martensite and the thermal/ mechanical controlled martensite-austenite transformation. The change of the modulus during the subsequent cooling process followed the reverse trend of its counterpart except the modulus at room temperature. The difference should be caused by the residual hardening during the heating-cooling cycle.

The dynamic characteristics of the SMA spring in transverse vibration were investigated using the experimental setup shown schematically in Fig. 3. The spring-mass system was excited in base vibration by a mechanical shaker. The excitation was

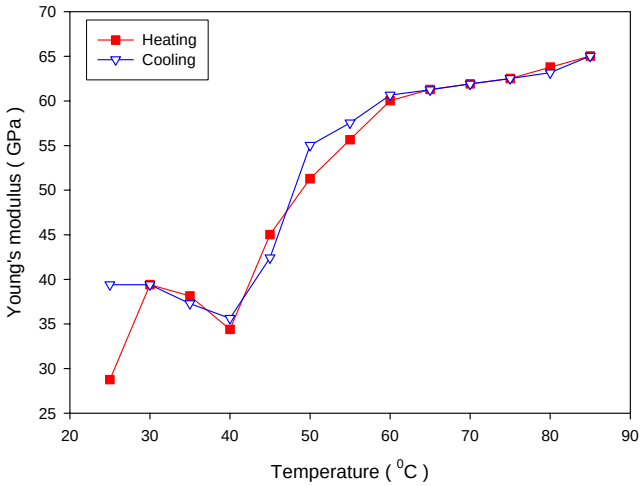

Figure 2 -- Apparent Young's modulus of the SMA spring at different temperatures

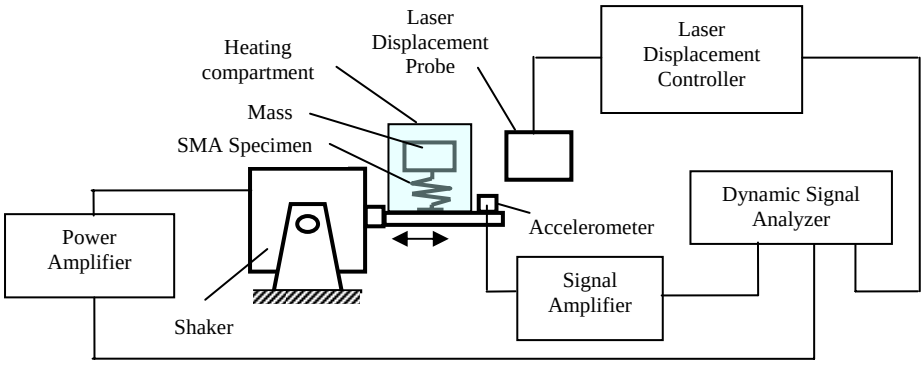

Figure 3 -- The schematic diagram of the test apparatus for dynamic measurement of SMA spring-mass system in transverse vibration

measured by the accelerometer mounted on the base while the resulted vibration displacement of the mass was detected by the laser displacement probe. Both the mass displacement and the base vibration were processed by the dynamic signal analyzer to find the resonance frequency of the system. The associated spring constant was then found using Eqn. (10). The temperature of the spring was controlled by the heating compartment encasing the system.

Figure 4 presents the change of the resonance frequency of the spring-mass system in transverse vibration at the heating and cooling process. The mass was 18.16*g* and the springs with 4, 5 and 6 numbers of active coil were employed. Similar to the results of static testing as shown in Fig. 2, the frequency reached a minimum at the temperature near 50°C. Except the first decrease at low temperature, the transformation of martensite to austenite during the heating process increased the modulus of the spring generally. A reverse trend was seen during the cooling process. However, the phase change during the cooling lagged that of heating. Therefore, the minimum frequency occurred at lower temperature for the cooling process.

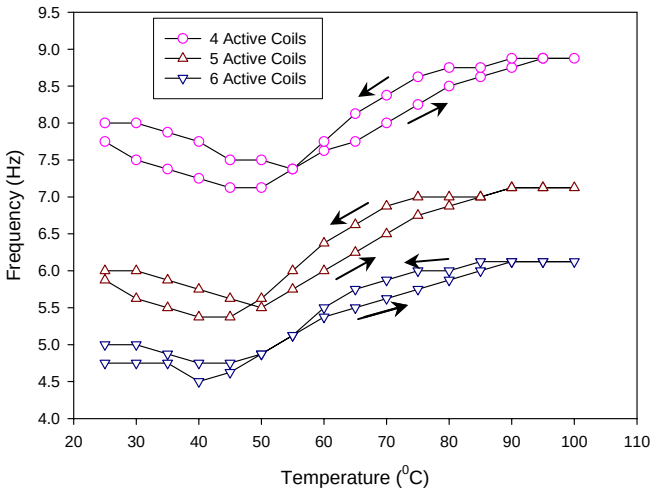

Figure 4 – The resonance frequency of the spring-mass system at the heating-cooling process

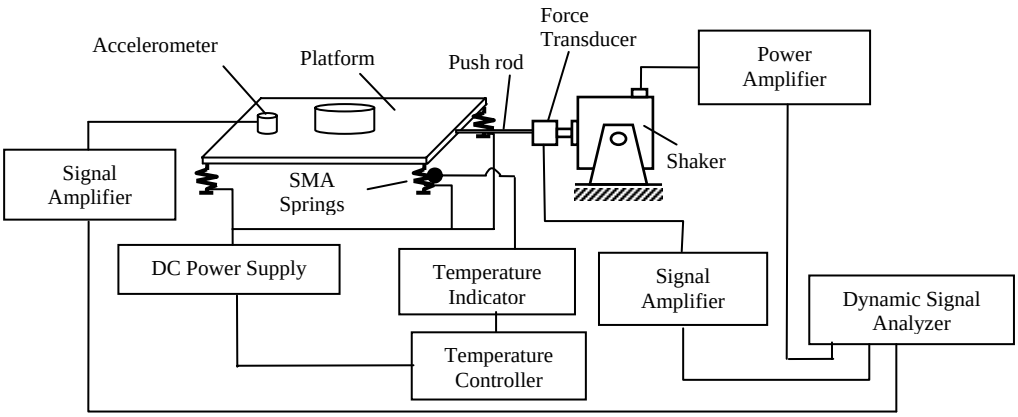

Figure 5 – The schematic diagram of the experimental setup for measuring the dynamic characteristics of the platform with SMA spring suspension

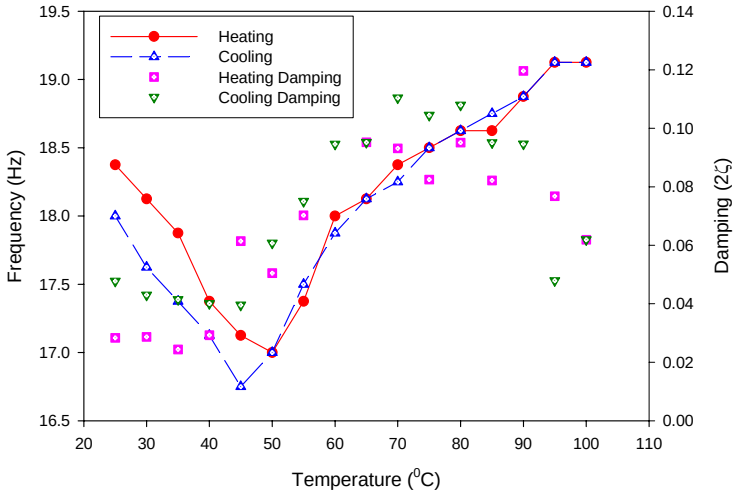

Figure 6 – The effect of temperature on the resonance frequency and damping of the platform with four SMA suspension springs excited in in-plane motion.

The schematic diagram of the experimental setup for measuring the dynamic characteristics of the platform with SMA spring suspension is shown in Fig. 5. The setup is similar to those of Fig. 3 except the spring-mass system had been replaced with the platform having four suspension SMA helical springs. Furthermore, the heating of the spring was controlled by adjusting the DC current supply. In addition to the resonance frequency, the damping capacity of the platform was also measured by using half-power-bandwidth method. The springs were all with 4 active coils and the acrylic platform was in dimensions of $10cm \times 15cm$ and weighted $300g$. The effect of the control temperature on the resonance frequency as shown in Fig. 6 was in the similar trend with the single spring system. However, the percentage in the change of the resonance frequency was within 14% and not as significant as the single spring system. On the other hand, the damping capacity of the system showed an obvious increase at

50°C, reached a maximum plateau, and then dropped to a smaller value as the temperature was near 100°C.

CONCLUSIONS

The change of the dynamic characteristics of the SMA helical spring due to the martensite-austenite transformation was investigated in this study. The derived spring constant under lateral deflection was shown to be consistent with that from the ANSYS simulation. The static compression test of the SMA spring showed the unusual decrease-then-increase trend in the spring constant during the heating process. From the dynamic test of the spring-mass system the same trend was also observed. This phenomenon should be obliged to both the phase transformation plateau and the associate modulus increment from martensite to austenite. A total 25% change in the resonance frequency of the spring-mass system within 25°C to 90°C temperature range demonstrated the controllability of the system. The test result of a platform with four SMA suspension springs showed the natural frequency for the in-plane vibration mode can be tuned from 6.5Hz to 8.5Hz by heating the spring from 45°C to 90°C. The theoretical modelling of the stress-strain curve under the influence of thermal control for the SMA material can be the topics for exploring the decrease-then-increase spring constant of the system.

ACKNOWLEDGEMENT

The partial financial support from NSC, Taiwan, under the Grant No. NSC 94-2745-E-212 -005-URD is greatly acknowledged.

REFERENCES

[1]. Huang, W. Y., Chao, C. P., Kang, J. R., and Sung, C. K., "The Application of Ball-Type Balancers for Radial Vibration Reduction of High-Speed Optic Disk Drives," Journal of Sound and Vibration, **250**(3), 415-430 (2001).

[2]. Takatoshi, Y., "Disk Drive Device," Japanese Patent 10,188,465 (1998).

[3]. Masaaki, K., "Disk Device," Japanese Patent 10,208,374 (1998).

[4]. Jinnouchi, Y., Araki, Y., Inoue, J., Ohtsuka, Y., and Tan, C., "Automatic Balancer (Static Balancing and Transient Response of a Multi-Ball Balancer)," Transactions of the Japan Society of Mechanical Engineers, Part C, **59**(557), 79-84 (1993).

[5]. Zhou, H. C., Lee, C. Y., and Sung, C. K., "The Study on the ER Suspension System Used in the Vibration Reduction of Optical Disk Drive," The Proceedings of the 13th R.O.C. Conference on the Vibration and Acoustics, June 5, Yuan-lin, Taiwan, Paper No. B9 (2005). (in Chinese)

[6]. Wong, W. H., Tse, P. C., Lau, K. J., Ng, Y. F., "Spring Constant of Fibre-reinforced Plastics Circular Springs Embedded with Nickel-Titanium Alloy Wire," Composite Structures, **65**, 319-328 (2004).

[7]. Williams, K., Chiu, G. and Bernhard, R., "Adaptive-Passive Absorbers Using Shape-Memory Alloys," Journal of Sound and Vibration, **249**, 835-848 (2002).

[8]. Liang, C. Rogers, C. A., "Design of Shape Memory Alloy Springs with Applications in Vibration Control," Journal of Vibration and Acoustics, **115**, 129-135 (1993).